J Mater Sci (2018) 53:8499–8509

Energy materials

Hierarchical bicomponent TiO_2 hollow spheres as a new high-capacity anode material for lithium-ion batteries

Ruiping Liu[1,2,3,*], Chao Shen[1], Chao Zhang[1], James Iocozzia[3], Qi Wang[1], Shiqiang Zhao[3], Kunjie Yuan[3], and Zhiqun Lin[3,*]

[1] Department of Materials Science and Engineering, China University of Mining and Technology (Beijing), Beijing 100083, China
[2] State Key Laboratory of Coal Resources and Safe Mining, China University of Mining and Technology (Beijing), Beijing 100083, China
[3] School of Materials Science and Engineering, Georgia Institute of Technology, Atlanta, GA 30332, USA

Received: 3 January 2018
Accepted: 2 March 2018
Published online: 9 March 2018

ABSTRACT

Hierarchical TiO_2-based hollow spheres were successfully synthesized via a hydrothermal method using $FeSO_4{\cdot}7H_2O$, $CoSO_4{\cdot}7H_2O$ and $ZnSO_4{\cdot}7H_2O$ as soft templates. The as-prepared hollow spheres are well dispersed with the diameters of 2–4 μm. The shell and the interior surface of the spheres are composed of loosely packed grains, which provide a large specific surface area to facilitate lithium-ion diffusion processes. Among the three types of hybrid hollow spheres, TiO_2/Fe_2O_3 shows the highest reversible capacity and best cycling stability (discharge capacities of 290.8 and 210.5 mAh/g were achieved after 100 cycles at 0.1C and 1C, respectively) and rate performance (from 461.1 mAh/g at 0.1C to 79.3 mAh/g at 5C with recovery to 288.6 mAh/g at 0.1C) for anode materials in lithium-ion batteries.

Introduction

Ever increasing demands for energy have led to staggering rates of fossil fuel consumption and corresponding high rates of harmful emissions. With established and mounting concerns over climate change, efforts have been dedicated to developing new energy storage devices for renewable and clean energy technologies. As one of the most promising energy storage technologies, lithium-ion batteries (LIBs) are widely used as a convenient power source for various portable electronics and electric vehicles (EV) due to their superior properties including relatively high-power density, long cycling life and environmental friendliness [1–4]. However, the limited energy density of lithium-ion batteries restricts their wider application in a variety of emerging vehicles. The energy density of a battery depends heavily on the output voltage and electrode theoretical capacity [5, 6]. It is well known that improvements in cathode performance are far more challenging when compared to anodes.

Address correspondence to E-mail: bjlrp165@126.com; 201402@cumtb.edu.cn; zhiqun.lin@mse.gatech.edu

https://doi.org/10.1007/s10853-018-2195-6

Consequently, anode development is one of the most important and accessible factors for improving LIB energy density and safety [7–9].

Compared to the commercial graphite-based anode materials with relative low theoretical capacity (372 mAh/g) and safety concerns, metal oxides such as TiO_2 [10], Fe_3O_4 [11], Co_3O_4 [12], SnO_2 [13, 14], NiO [15] and MnO [16] are promising candidates for the use in lithium-ion batteries due to their relatively high theoretical capacity, stable reversible capacity and safety. However, many metal oxides suffer from the large volume changes (> 300%) during charging and discharging leading to pulverization and delamination of the anode ultimately leading to poor cycling performance [17, 18]. In addition, the poor electrical conductivity of the metal oxides typically leads to electrodes with poor rate capacity [19, 20]. Among the various metal oxides, TiO_2 has received particular interest as a promising battery anode candidate because of its low capacity loss, high-power capability, low cost, abundance and environmental friendliness [21]. Furthermore, the relatively small volume change (< 4%) during charging and discharging helps to preserve the electrode structure enabling prolonged cycling life. Although the working potential of TiO_2 is a little high to be used as an anode material, it remains an attractive option due to its electrochemical stability in common organic electrolytes which leads to an improved overcharge protection and overall improved battery safety [22].

The electrochemical properties of TiO_2 electrodes heavily depend on their composition, microstructure, crystallinity and crystallite size. It is well known that nanostructured materials possess enhanced cycling and rate performance. Nanostructured TiO_2 with different morphologies, such as nanoparticles [23, 24], nanorods [25], nanotubes [26], nanowires [27], nanosheets [28] and nanospheres [29, 30], has been successfully synthesized, and the electrochemical properties extensively investigated. However, the poor electronic conductivity (10^{-12}–10^{-7} S/cm), the frequent aggregation of TiO_2 nanoparticles and the low Li^+ diffusion rate (10^{-15}–10^{-9} cm^2/s) often hinder the electrochemical performance of TiO_2-based electrodes. In order to improve the electric conductivity, carbonaceous materials such as amorphous carbon [31], carbon nanotubes [32] and graphene [33] are often used to form either a mixture with TiO_2 or a thin coating layer on its surface. Despite the advantages of adding carbon, its introduction into TiO_2 can reduce the amount of active materials in the electrode resulting in a reduced mass energy density and volume energy density of resulting batteries. Recently, many works focused on fabricating TiO_2-based composite as anode materials for LIBs in order to improve the electrochemical performance of TiO_2 by utilizing the synergistic effect between TiO_2 and other metal oxides, such as Fe_2O_3 [34], Nb_2O_5 [35], CoO [36], SnO_2 [37], $NiCo_2O_4$ [38]. Among them, due to the high theoretical capacity of Fe_2O_3 (1005 mAh/g), Co_2O_3 (890 mAh/g) and ZnO (981 mAh/g), they show great prospect toward high-energy anodes, and it can be deduced that the capacity will be largely improved by preparing TiO_2-based composites with the above three metal oxides due to their synergistic effect. Moreover, due to their conversion reaction mechanisms during cycling, the metal oxide will be reduced to metal first, which will improve the electrical conductivity of the TiO_2-based anode materials, and finally enhance the electrochemical performance.

Herein, we present bicomponent porous hierarchical TiO_2 spheres for facilitating lithium-ion diffusion through active materials by enlarging the contact area between the liquid electrolyte and the active materials. In addition, a second phase of metal oxide was introduced to the TiO_2 grains by a one-step hydrothermal method using hydrated metal sulfates as soft templates. The ZnO, Fe_2O_3 and Co_2O_3 will react with lithium ions to form the corresponding Zn, Fe and Co and Li_2O during charging first, which may facilitate electron and ion transfer during cycling and thus may also improve the electrochemical performance of the TiO_2 as anode materials in lithium-ion batteries.

Experimental

Synthesis of TiO_2 hybrid hollow spheres

In a typical synthesis procedure, 1 g of $FeSO_4{\cdot}7H_2O$, $CoSO_4{\cdot}7H_2O$ or $ZnSO_4{\cdot}7H_2O$ was added to anhydrous ethanol (60 ml) under continuous stirring for 1 h to form a white suspension. Tetrabutyl titanate (TBT) (4 ml) was then added to the suspension over 20 min. The mixture was stirred for 1 h and transferred to a 100-mL Teflon-sealed autoclave maintained at 200 °C for 24 h. The resulting precipitates were separated and purified by centrifugation and washed three times with DI water and ethanol.

Samples were then dried in a vacuum oven at 70 °C for 5 h to yield hierarchical porous TiO_2/Fe_2O_3, TiO_2/CO_2O_3 and TiO_2/ZnO hybrid hollow spheres.

Characterization

X-ray diffraction (XRD) patterns were measured on a Bruker D8 Advance diffractometer using Ni-filtered Cu Kα radiation. The morphologies of the as-prepared bicomponent hierarchical porous hollow spheres were observed by SEM (Carl Zeiss Jena scanning microscope) and TEM (JEOL JEM-2011). Brunner – Emmet – Teller (BET) surface area was measured by N_2 adsorption at liquid nitrogen temperature using a NOVA4000 automated gas sorption system. X-ray photoelectron spectroscopy (XPS) (ESCALAB 250XI) was used to further verify the chemical composition of the samples.

Electrochemical measurements

In order to further evaluate the electrochemical performance of the as-prepared TiO_2/Fe_2O_3, TiO_2/CO_2O_3 and TiO_2/ZnO hollow spheres as anode materials in lithium-ion batteries, CR2032 coin-type cells were assembled in a glove box (Mikrouna, Shanghai, China) filled with high-purity Ar. Neat lithium metal foil was used as both the counter and reference electrodes, polypropylene microporous film (Celgard 2400) was used as a separator, and a 1-M $LiPF_6$ dissolved in a mixture of ethylene carbonate (EC), diethyl carbonate (DEC) and dimethyl carbonate (DMC) (1:1:1 by volume) served as the electrolyte. The working electrodes were fabricated by mixing the active material (TiO_2/Fe_2O_3, TiO_2/CO_2O_3 or TiO_2/ZnO hybrid hollow spheres), carbon black and polyvinylidene fluoride (PVDF) in a weight ratio of 75: 15: 10. The slurry was uniformly spread on Cu foil and dried at 110 °C for 12 h in vacuum. The cells were cycled between 0.001 and 2.5 V (vs. Li/Li^+) at current densities from 0.1C to 5C at room temperature. Cyclic voltammetry (CV) and electrochemical impedance spectroscopy (EIS) were carried out on an electrochemical workstation (CHI660C, Shanghai Chenhua). The CV was performed at a scan rate of 0.1 mV/s. EIS measurements were recorded over a frequency range of 100 kHz to 0.01 Hz.

Results and discussion

The overall synthesis strategy is illustrated in Scheme 1. First, hydrated sulfate templates were formed by dispersing hydrated sulfates in anhydrous ethanol solution with appropriate stirring speed at which time the hydrated sulfate particles aggregate to form spheres. With the slow addition of tetrabutyl titanate, uniform solutions are obtained. The hydrolysis of tetrabutyl titanate to form TiO_2 nanocrystallites is triggered by the slow release of water from the hydrated sulfates during hydrothermal treatment. Hollow TiO_2 spheres were obtained by removing the templates during the washing stage.

Figure 1 shows SEM images of TiO_2 hybrid hollow spheres prepared using different templates. The bicomponent TiO_2 hollow spheres with diameters in the range of 2–4 μm exhibit well-developed spherical morphologies (Fig. 1a–c). SEM images of the TiO_2 spheres clearly show their hollow structure (Fig. 1d–f). The hollow structure is further supported through TEM imaging (Fig. 2) in which a clear contrast between the edge and the center of the TiO_2 hollow spheres can be observed. Figure 1e, f shows that the hollow spheres possess a rough internal surface and loosely packed shell which confer high specific surface area. These features are also indicative of the spherical hydrated sulfate templates used in the TiO_2 sphere formation while also providing additional evidence for the proposed growth mechanism.

The XRD patterns of the as-prepared hybrid hollow spheres are shown in Fig. 3. It can be seen that regardless of the hydrated sulfate used as a template,

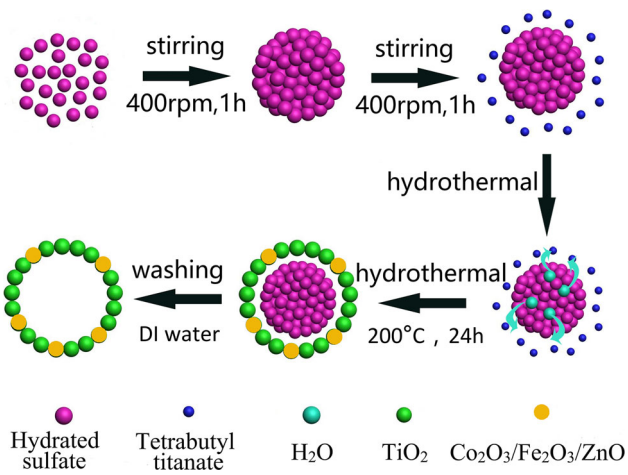

Scheme 1 The synthesis strategy of the TiO_2 hybrid hollow spheres.

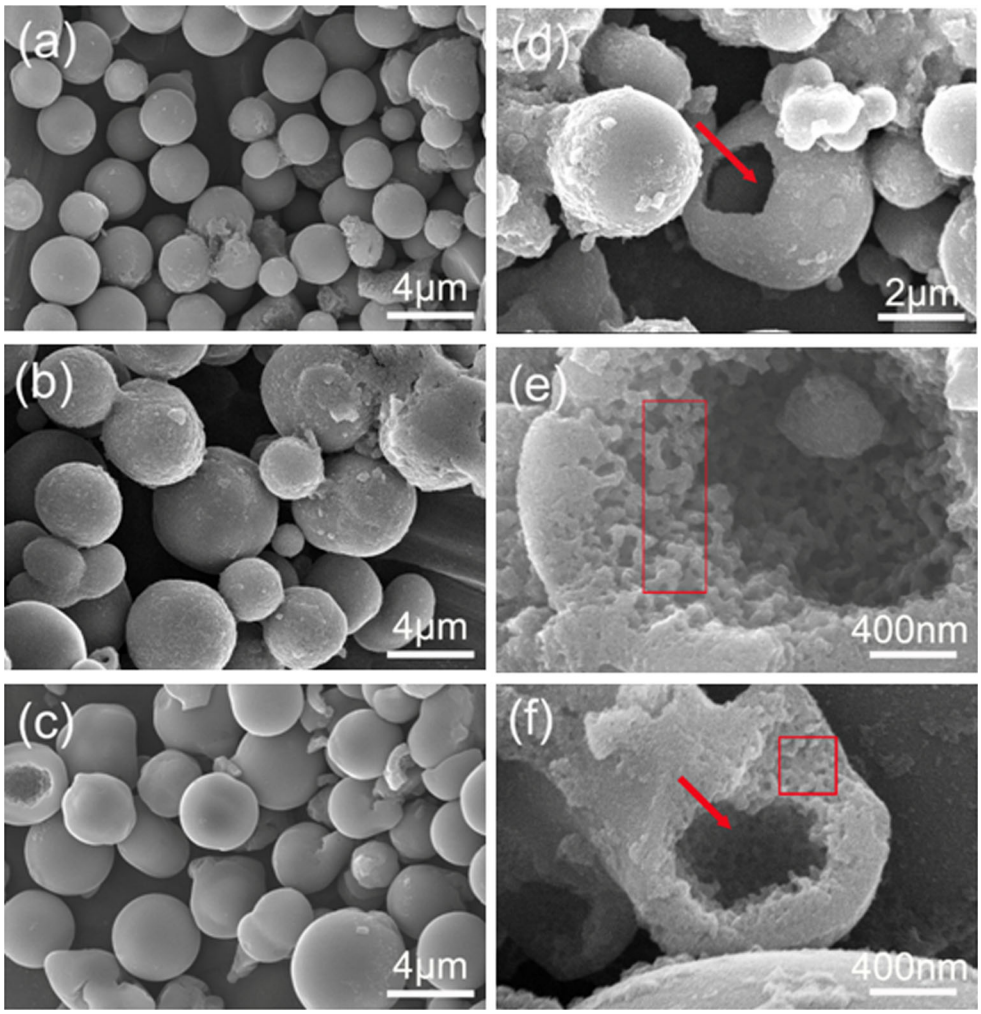

Figure 1 SEM images of bicomponent hollow spheres prepared by hydrated sulfate templating **a**, **d** TiO_2/Fe_2O_3, **b**, **e** TiO_2/CO_2O_3 and **c**, **f** TiO_2/ZnO.

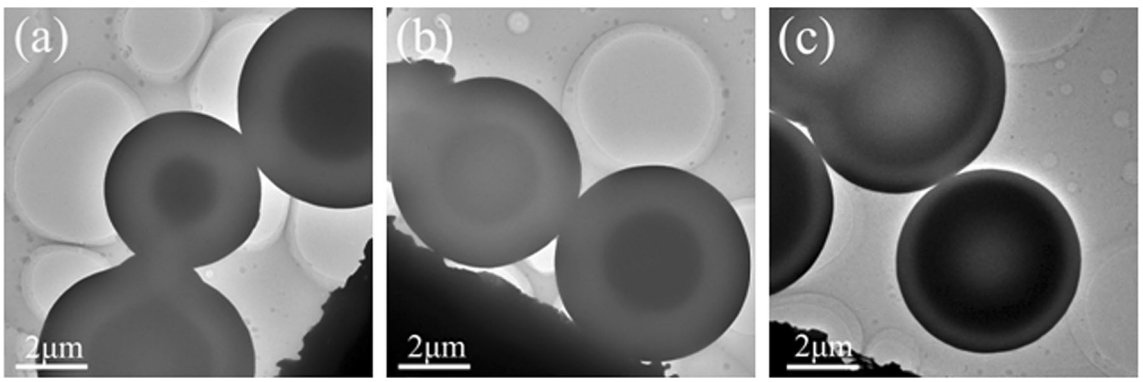

Figure 2 TEM images of the bicomponent hollow spheres **a** TiO_2/Fe_2O_3, **b** TiO_2/Co_2O_3 and **c** TiO_2/ZnO.

the diffraction peaks of the as-prepared materials could all be indexed to the anatase phase of TiO_2 (JCPDS Card No. 21-1272). Furthermore, no evidence of the template materials is observed, indicating successful removal of the template materials. The average TiO_2 crystallite size was calculated as 8.5 nm using the Debye–Scherrer equation [39].

The BET-specific surface area of the hierarchical porous TiO_2/Fe_2O_3 hybrid hollow spheres is $225.25 \pm 3.25\ m^2/g$. The inset in Fig. 4 shows the

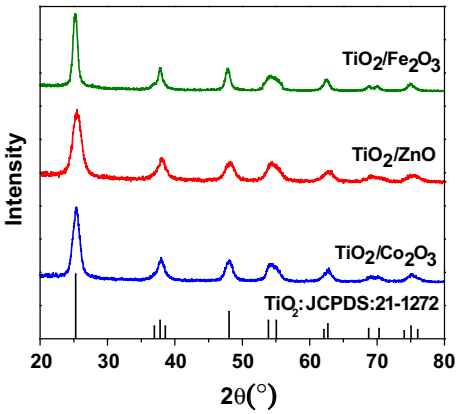

Figure 3 XRD patterns of the as-prepared hybrid hollow spheres templated by different hydrated sulfates. The JCPDS 21-1272 is corresponding to the anatase TiO_2.

pore size distribution for the hollow TiO_2/Fe_2O_3 spheres, and the Barrett–Joyner–Halenda (BJH) mesopore size distribution of the sample exhibits a sharp peak centered at 3.95 nm. This indicates a relatively uniform mesopore size throughout the hollow TiO_2 shell. For hollow TiO_2/Co_2O_3 and TiO_2/ZnO spheres, the BET measurements also show narrow pore size distributions with average sizes of 3.82 nm and 3.85 nm and large specific surface areas of 220.69 ± 2.67 m^2/g and 223.54 ± 3.58 m^2/g, respectively. The consistency of the observed pore sizes and high surface areas across several different metal sulfate hydrates suggests that a hydrated sulfate-assisted hydrothermal method is an ideal templating approach. Both the high specific surface area and hierarchical porous structure of the hybrid spheres are likely contributors to the improved electrochemical performance of lithium-ion battery anode materials during the charge/discharge process as they provide large contact areas for the liquid electrolyte and active materials while also shortening the ion diffusion distance.

In order to further determine the chemical environment of Zn, Fe and Co in the bicomponent materials, XPS was performed (Fig. 5). It can be seen that the Ti 2p XPS spectrum can be fitted with a single

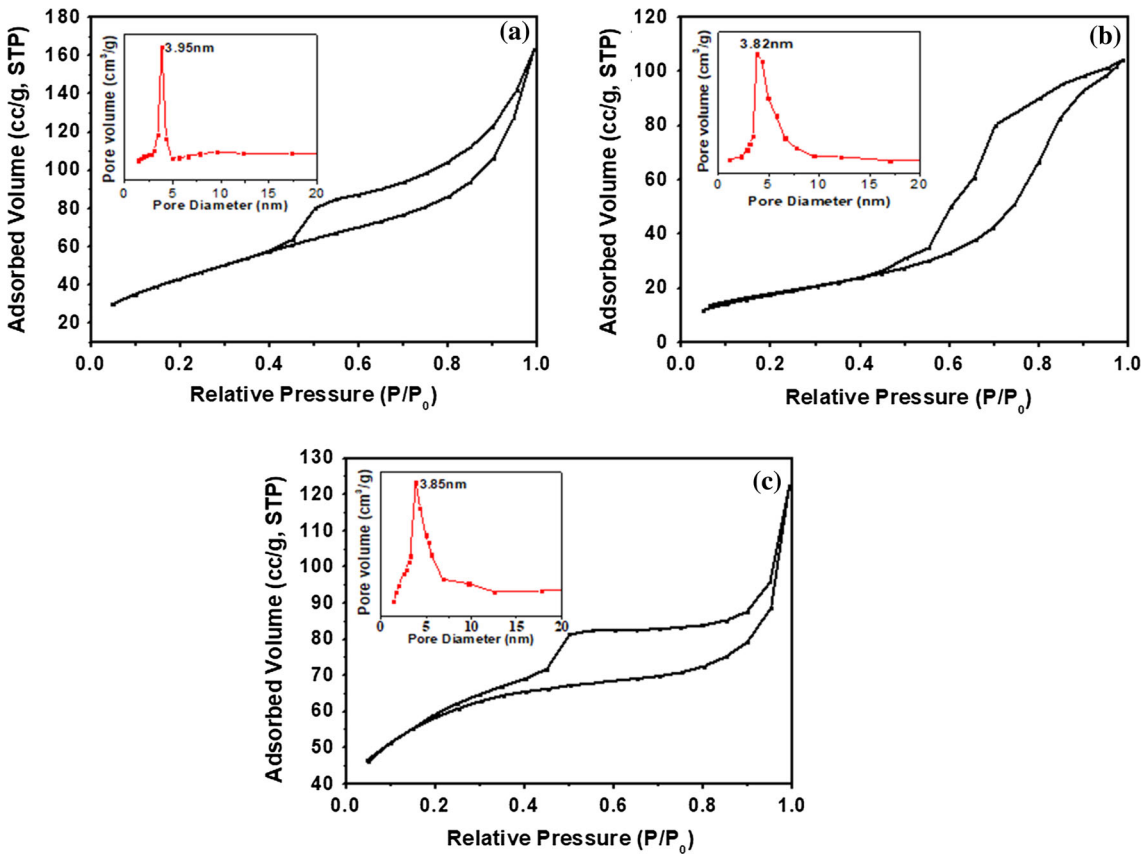

Figure 4 N_2 adsorption–desorption isotherms and pore size distributions (inset) of TiO_2/Fe_2O_3 (**a**), $TiO_2//Co_2O_3$ (**b**) and TiO_2/ZnO (**c**) hollow spheres.

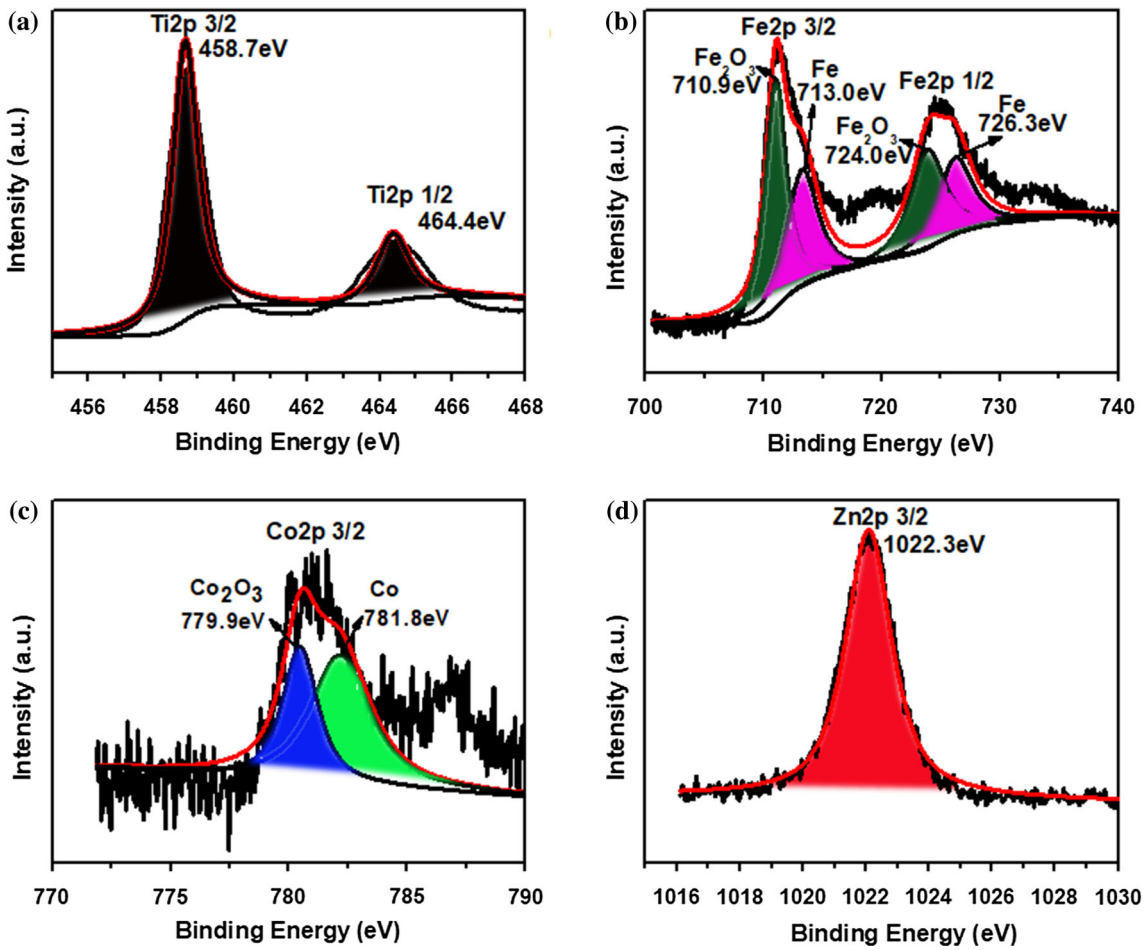

Figure 5 XPS spectrum of the Ti (**a**), Fe (**b**), Co (**c**) and Zn (**d**) in the hybrid materials, raw data (black line) and fitted data (red line).

peak corresponding to TiO_2 (Fig. 5a), and the Zn 2p XPS spectrum can be fitted with a single peak with a binding energy of 1022.3 eV (Fig. 5c) corresponding to ZnO. In contrast, for bicomponent TiO_2/Fe_2O_3, the Fe 2p 1/2 and 3/2 XPS spectrum can be fitted with two peaks, respectively, and indexed to Fe_2O_3 and Fe (Fig. 5b). The Co 2p XPS spectrum can be fitted with two peaks indicating the existence of Co_2O_3 and Co in bicomponent TiO_2/CO_2O_3 as expected. XPS results further confirm that the desired bicomponent materials can be obtained by the above one-step hydrothermal method.

Coin cells were assembled to evaluate the performance of the bicomponent TiO_2 hollow spheres as anodes in lithium-ion batteries. The first three CV curves of the hybrid spheres are presented in Fig. 6. In the first cathodic sweep, the lithium-ion insertion potentials are 1.42 V, 1.56 V and 1.57 V vs. Li/Li^+ for TiO_2/Fe_2O_3, TiO_2/CO_2O_3 and TiO_2/ZnO bicomponent hollow spheres, respectively. This corresponds to the reduction of Ti^{4+} to Ti^{3+} [39]. The subsequent oxidation process occurs at 2.22 V, 2.16 V and 2.18 V vs. Li/Li^+ for TiO_2/Fe_2O_3, TiO_2/CO_2O_3 and TiO_2/ZnO bicomponent hollow spheres. After the first cycle, the cathodic peak potentials of the three materials all shift to the higher voltage region. In contrast, the anodic peak shifts to the lower voltage region. This suggests a reduced anode polarization and increased Li^+ insert/extraction reversibility during electrochemical cycling. Concurrently, the corresponding current peaks decrease revealing the existence of an irreversible capacity loss in the initial lithiation–delithiation process. The insertion and extraction of lithium ions into and from the TiO_2 lattice can be described as follows:

$$TiO_2 + xLi^+ + xe^- \leftrightarrow Li_xTiO_2$$

It can also be seen that unlike the CV curves of TiO_2/CO_2O_3 (Fig. 6a) and TiO_2/ZnO hybrid hollow spheres (Fig. 6c), there is a distinct cathodic peak for

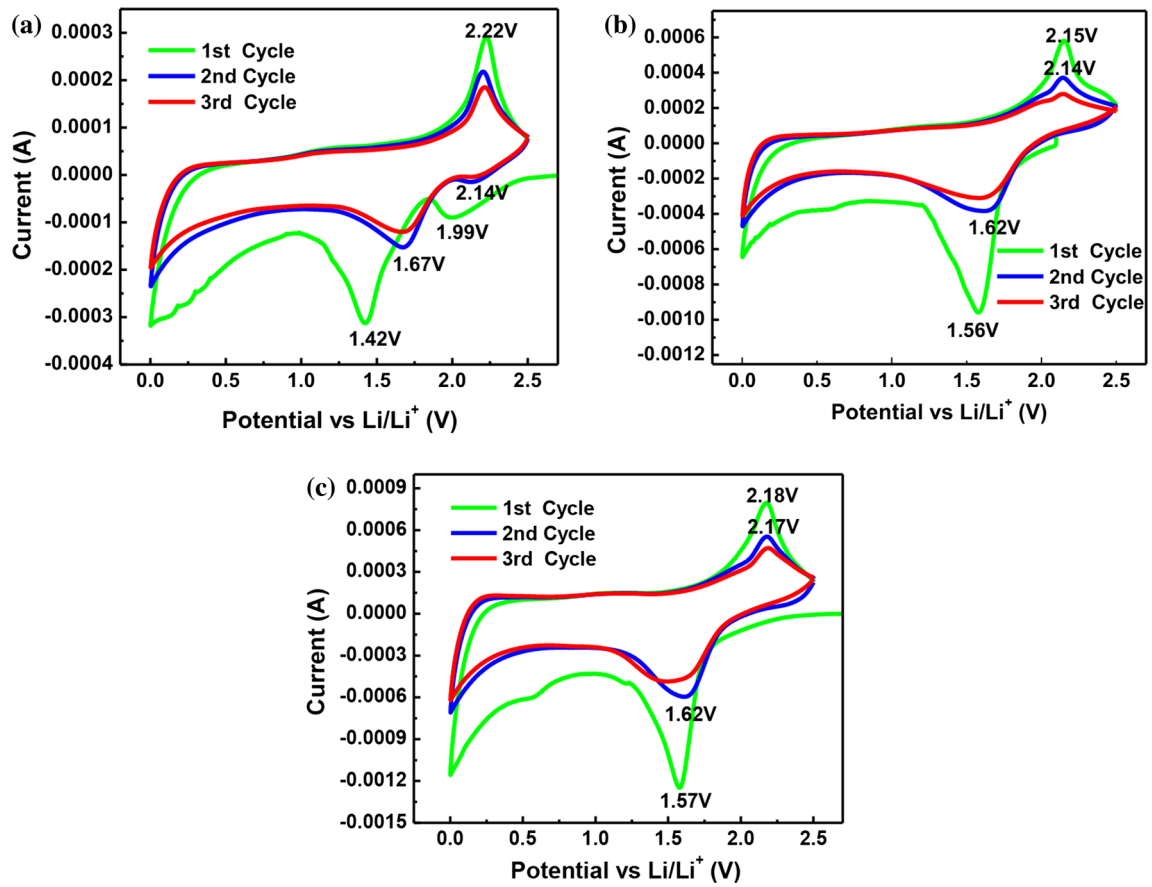

Figure 6 Cyclic voltammograms for the first (green), second (blue) and third (red) cycles for the TiO_2/Fe_2O_3 (**a**), TiO_2/CO_2O_3 (**b**) and TiO_2/ZnO (**c**) component spheres over the potential range of 0 V to 2.5 V vs. Li/Li^+ with a scan rate of 0.1 mV s^{-1}.

the TiO_2/Fe_2O_3 bicomponent hollow spheres (Fig. 6b). Located initially at 1.99 V in the first cycle, the peak moved to the higher voltage region (2.14 V) in the second and third cycle. This observation may be attributed to lithium insertion into the crystal structure of Fe_2O_3 without a significant change in the structure [40]. This would enable an improved lithium-ion storage capability of the bimetallic hollow spheres by essentially providing more sites for lithium uptake. It is noteworthy that the second and third cycles of the voltage–current curves for all three samples almost overlap with each other. This suggests good reversibility and stability of the electrochemical reaction after the first cycle.

Figure 7 presents the cycling and rate performance of the bicomponent hollow spheres. The TiO_2/Fe_2O_3, TiO_2/CO_2O_3 and TiO_2/ZnO hollow spheres deliver discharge capacities of 288.6, 180.3 and 221.1 mAh/g, respectively, after 100 cycles at a current density of 0.1C. At a current density of 1C, the hybrid hollow spheres also exhibit stable cycling performance. It can be seen that the discharge capacity of the three electrodes slightly decreases in the first 10 cycles and then gradually stabilized during the following 90 cycles with a Coulombic efficiency of 99%. After 100 charge–discharge cycles, the TiO_2/Fe_2O_3, TiO_2/CO_2O_3 and TiO_2/ZnO bicomponent hollow spheres still deliver discharge capacity of 210.5, 78.6 and 177.7 mAh/g, respectively. These sustained performance values suggest that bicomponent hollow spheres are promising anode materials even when subjected to large current densities (Fig. 7b). Figure 7c presents the rate capability of the bicomponent hollow spheres at various current rates from 0.1C to 5C (1C = 335 mAh/g). The capacity values are the averaged over 10 cycles. As expected, the capacity gradually decreases as the current rate increases. It can be seen that among the three bicomponent hollow spheres, the TiO_2/Fe_2O_3 hollow spheres show the best rate performance with the rate performance of the TiO_2/CO_2O_3 and TiO_2/ZnO hollow spheres being comparable. For TiO_2/Fe_2O_3 hollow spheres,

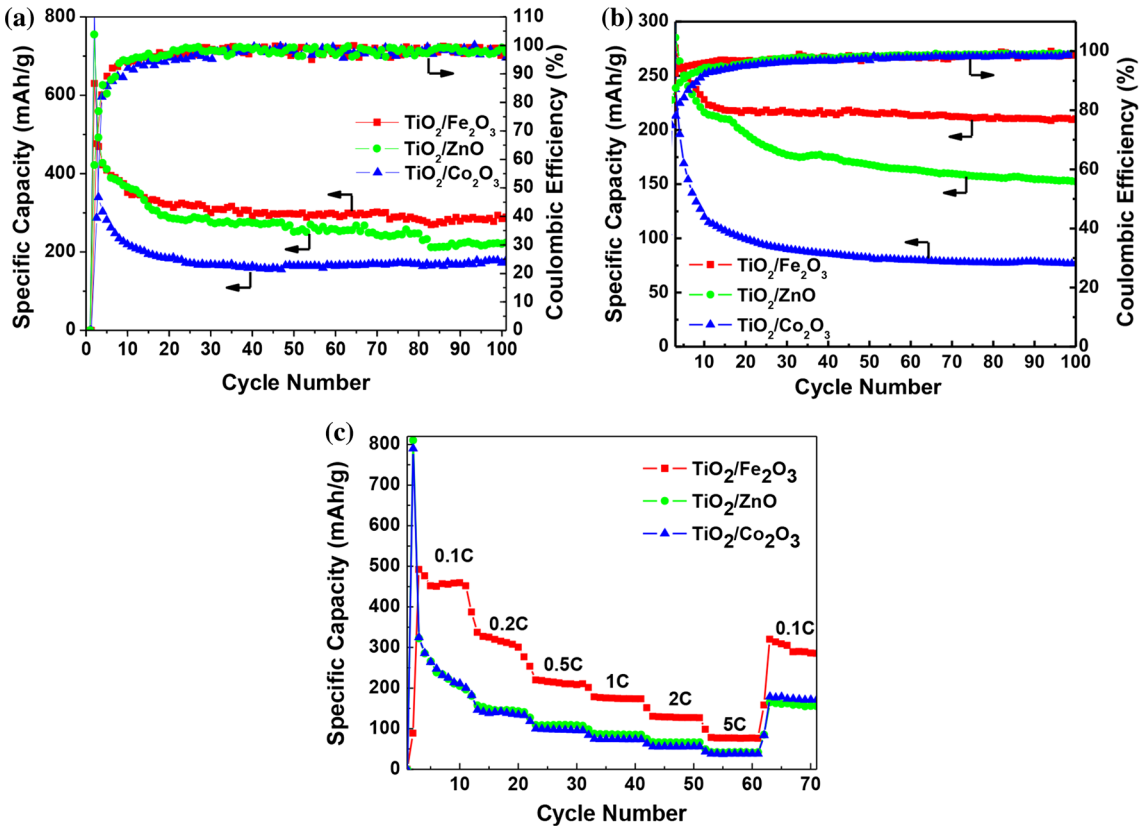

Figure 7 Cycling performance at a current density of 0.1C (**a**) and 1C (**b**), rate performance of bicomponent hollow materials (**c**): TiO_2/Fe_2O_3 (red), TiO_2/CO_2O_3 (blue) and TiO_2/ZnO (green).

the reversible capacity of the electrode after 50 cycles is 461.1, 307.8, 212.8, 174.3, 127.7 and 79.3 mAh/g for current densities of 0.1C, 0.2C, 0.5C, 1C, 2C and 5C, respectively. More importantly, when the current density returns to 0.1C, a capacity of 288.6 mAh/g can be recovered. This confirms the good rate performance and stability of the bicomponent hollow spheres. Despite TiO_2/Co_2O_3 and TiO_2/ZnO hollow spheres possessing lower overall performance values across all current densities, a relatively high discharge capacity can still be recovered by reducing the current density to 0.1C. This observation suggests that the additional metal oxides play the same role in these systems. It is noted that the initial capacity of the three types of hybrid hollow spheres is more than 600 mAh/g, much higher than that of TiO_2. The extra capacity may be due to synergistic effect between TiO_2 and three different metal oxides. Firstly, as we all known that the theoretical capacity of Fe_2O_3, Co_2O_3 and ZnO is much higher than that of TiO_2, during cycling, the metal oxide will be reduced to metal first, and then, metal will react with lithium to form alloy, which will contribute more capacity. Secondly, according to Ref. [41], the extra capacity may be due to the further lithium storage via interfacial reaction between the metal and Li_2O phase boundary. And thirdly, the reduced metal may improve the electrical conductivity of the anode, which will further improve the rate performance of the anode.

In order to further understand the enhanced electrochemical performance of the bicomponent hollow spheres, electrochemical impedance spectroscopy (EIS) was used to evaluate the impedance and lithium-ion diffusion rate. As shown in Fig. 8, the EIS spectra are presented in the typical Nyquist plots format showing a semicircle at the high-medium frequency region which can be attributed to the ohmic resistance (R_s) and the charge-transfer resistance at the interface between the electrode and electrolyte (R_{ct}). The sloping line in the low frequency region corresponds to lithium-ion diffusion in the solid electrode [42]. The Nyquist plots are fitted by using equivalent circuit modeling [43]. In the

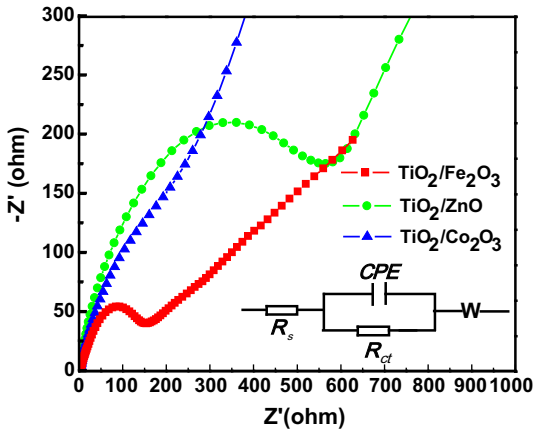

Fig. 8 Nyquist plots of the hollow bicomponent spheres. Inset shows the equivalent circuit used to fit the experimental impedance spectra data.

equivalent circuit (inset), R_s and R_{ct} are the ohmic resistance and the charge-transfer resistance of the electrodes. The constant phase-angle element (CPE) and the Warburg impedance (W) indicate the lithium-ion diffusion into the bulk active material. The diameters of the resistance arcs for the TiO_2/Fe_2O_3 electrode are much smaller than those for TiO_2/CO_2O_3 and TiO_2/ZnO electrodes. This indicates that the TiO_2/Fe_2O_3 electrode exhibits a lower surface film resistance and charge-transfer resistance. According to the fitting results (Table 1), the R_s, R_{ct} and W of the TiO_2/Fe_2O_3 bicomponent hollow spheres are smaller than those of TiO_2/CO_2O_3 and TiO_2/ZnO. These results suggest that the electrical conductivity, charge-transfer kinetics and diffusion of lithium ions can be effectively improved by combining TiO_2 and Fe_2O_3.

Conclusions

Bicomponent TiO_2 hollow spheres have been successfully synthesized under hydrothermal conditions using different hydrated sulfates as template. The resulting structures are composed of both TiO_2 and the corresponding metal oxide derived from the hydrated sulfate template. The bicomponent hollow spheres are well developed and distinct with a diameter of 2–4 μm. The rough interior surface and loose grain-packed shells afford the hollow spheres large specific surface areas for facilitating lithium-ion diffusion during charging and discharging. These bicomponent hollow spheres can greatly improve the electrochemical properties of TiO_2. The composition of the hybrid spheres also has a significant impact on the electrochemical performance of the electrode. The attractive properties and one-step synthesis method make the TiO_2 bicomponent hollow spheres a promising anode material for lithium-ion batteries.

Table 1 Impedance parameters for bicomponent hollow spheres

Samples	TiO_2/Fe_2O_3	TiO_2/CO_2O_3	TiO_2/ZnO
R_s (Ω)	0.981	8.72	1.437
R_{ct} (Ω)	96.39	130.2	687.7
CPE	7.13	3.07	1.41
W	401.72	3987	6425

Acknowledgements

This work was supported by the National Natural Science Foundation of China (NSFC No. 51202117), Natural Science Foundation of Beijing (No. 2162037), the Beijing Nova Program (Z171100001117077), the Beijing Outstanding Talent Program (No. 2015000020124G121), the Fundamental Research Funds for the Central Universities (No. 2014QJ02), the State Key Laboratory of Coal Resources and Safe Mining (No. SKLCRSM16KFB04) and the Yue Qi Young Scholar Project of China University of Mining & Technology, Beijing.

Author contributions

R.P.L and Z.Q.L managed the projects and guided the research. C.S and C.Z conducted all experiments. J.I, Q.W, S.Q.Z and K.J.Y performed the data analysis. R.P.L and Z.Q.L conceived the storyline of the paper. All authors contributed to the discussions and wrote the paper.

Compliance with ethical standards

Conflict of interest The authors declare that they have no conflict interest.

References

[1] Arico AS, Bruce P, Scrosati B, Tarascon JM, Van Schalkwijk W (2005) Nanostructured materials for advanced energy conversion and storage devices. Nat Mater 4:366

[2] Scrosati B, Garche J (2010) Lithium batteries: status, prospects and future. J Power Sources 195:2419
[3] Manthiram A (2011) Materials challenges and opportunities of lithium ion batteries. J Phys Chem Lett 2:176
[4] Goodenough JB, Park KS (2013) The li-ion rechargeable battery: a perspective. J Am Chem Soc 135:1167
[5] Chen JJ (2013) Recent progress in advanced materials for lithium ion batteries. Materials 6:156
[6] Croguennec L, Palacin MR (2015) Recent achievements on inorganic electrode materials for lithium-ion batteries. J Am Chem Soc 137:3140
[7] Roy P, Srivastava SK (2015) Nanostructured anode materials for lithium ion batteries. J Mater Chem A 3:2454
[8] Ji LW, Lin Z, Alcoutlabi M, Zhang XW (2011) Recent developments in nanostructured anode materials for rechargeable lithium-ion batteries. Energy Environ Sci 4:2682
[9] Lee WW, Lee JM (2014) Novel synthesis of high performance anode materials for lithium-ion batteries (LIBs). J Mater Chem A 2:1589
[10] Chen Y, Ma XQ, Cui XL, Jiang ZY (2016) In situ synthesis of carbon incorporated TiO_2 with long-term performance as anode for lithium-ion batteries. J Power Sources 302:233
[11] Wang JX, Wang G, Wang H (2015) Flexible free-standing Fe_2O_3/graphene/carbon nanotubes hybrid films as anode materials for high performance lithium-ion batteries. Electrochim Acta 182:192
[12] Fang ZG, Xu WW, Huang T et al (2013) Facile scalable synthesis of Co_3O_4/carbon nanotube hybrids as superior anode materials for lithium-ion batteries. Mater Res Bull 48:4419
[13] Deng YF, Fang CC, Chen GH (2016) The developments of SnO_2/graphene nanocomposites as anode materials for high performance lithium ion batteries: a review. J Power Sources 304:81
[14] Liu RP, Su WM, He P et al (2016) Synthesis of SnO_2/Sn hybrid hollow spheres as high performance anode materials for lithium ion battery. J Alloy Compd 688:908
[15] Pang YP, Zhang J, Chen DR, Jiao XL (2016) 3D hierarchical porous NiO nanoflowers as an advanced anode material with remarkable lithium storage performance. Rsc Adv 6:30395
[16] Xiao Y, Cao MH (2015) Carbon-anchored MnO nanosheets as an anode for high-rate and long-life lithium-ion batteries. ACS Appl Mater Interfaces 7:12840
[17] Yuan S, Ma DL, Wang S, Liu YB, Yang XH, Cao ZY (2015) Hierarchical porous SnO_2/Mn_2O_3 core/shell microspheres as advanced anode materials for lithium-ion batteries. Mater Lett 145:104
[18] Dong YC, Md K, Chui YS et al (2015) Synthesis of CNT@Fe_3O_4-C hybrid nanocables as anode materials with enhanced electrochemical performance for lithium ion batteries. Electrochim Acta 176:1332
[19] Tian QH, Tian Y, Zhang ZX, Yang L, Hirano S (2015) Fabrication of CNT@void@SnO_2@C with tube-in-tube nanostructure as high-performance anode for lithium-ion batteries. J Power Sources 291:173
[20] Li Y, Yu SL, Yuan TZ, Yan M, Jiang YZ (2015) Rational design of metal oxide nanocomposite anodes for advanced lithium ion batteries. J Power Sources 282:1
[21] Han CP, Yang D, Yang YK et al (2015) Hollow titanium dioxide spheres as anode material for lithium ion battery with largely improved rate stability and cycle performance by suppressing the formation of solid electrolyte interface layer. J Mater Chem A 3:13340
[22] Nuspl G, Yoshizawa K, Yamabe T (1997) Lithium intercalation in TiO_2 modifications. J Mater Chem 7:2529
[23] Yan JY, Song HH, Yang SB, Yan JD, Chen XH (2008) Preparation and electrochemical properties of composites of carbon nanotubes loaded with Ag and TiO_2 nanoparticle for use as anode material in lithium-ion batteries. Electrochim Acta 53:6351
[24] Wang MY, Pang XC, Zheng DJ et al (2016) Nonepitaxial growth of uniform and precisely size-tunable core/shell nanoparticles and their enhanced plasmon-driven photocatalysis. J Mater Chem A 4:7190
[25] Lee JH, Hon MH, Chung YW, Leu IC (2011) The effect of TiO_2 coating on the electrochemical performance of ZnO nanorod as the anode material for lithium-ion battery. Appl Phys Mater Sci Process 102:545
[26] Zhang MH, Yin KB, Hood ZD et al (2017) In situ TEM observation of the electrochemical lithiation of N-doped anatase TiO_2 nanotubes as anodes for lithium-ion batteries. J Mater Chem A 5:20651
[27] Tang YP, Tan XX, Hou GY, Cao HZ, Zheng GQ (2012) Synthesis of dense nanocavities inside TiO_2 nanowire array and its electrochemical properties as a three-dimensional anode material for Li-ion batteries. Electrochim Acta 78:154
[28] Wu FX, Wang ZX, Li XH, Guo HJ (2014) Simple preparation of petal-like TiO_2 nanosheets as anode materials for lithium-ion batteries. Ceram Int 40:16805
[29] Qiao Y, Hu XL, Liu Y, Liang G, Croft MC, Huang YH (2013) Surface modification of MoOxSy on porous TiO_2 nanospheres as an anode material with highly reversible and ultra-fast lithium storage properties. J Mater Chem A 1:15128
[30] Liang JC, Zhang XL, Zhai XJ, Zhang LJ, Wu WZ, Yu KF (2017) TiO_2 hollow spheres on reduced graphene oxide with high rate performance as anodes for lithium ion batteries. Rsc Adv 7:53097

[31] Park SJ, Kim YJ, Lee H (2011) Synthesis of carbon-coated TiO_2 nanotubes for high-power lithium-ion batteries. J Power Sources 196:5133

[32] Yan ZC, Liu L, Guo HP et al (2014) One-pot synthesis of FCNTs-wired TiO_2 nanocomposites as anode materials for high-rate lithium ion batteries. Electrochim Acta 123:551

[33] Zhen MM, Sun MQ, Gao GD, Liu L, Zhou Z (2015) Synthesis of mesoporous wall-structured TiO_2 on reduced graphene oxide nanosheets with high rate performance for lithium-ion batteries. Chem Eur J 21:5317

[34] Zhong Y, Ma YF, Guo QB et al (2017) Controllable synthesis of TiO_2@Fe_2O_3 core-shell nanotube arrays with double-wall coating as superb lithium-ion battery anodes. Sci Rep 7:40927

[35] Liu YB, Lin LW, Zhang WF, Wei MD (2017) Heterogeneous TiO2@Nb_2O_5 composite as a high-performance anode for lithium-ion batteries. Sci Rep 7:7204

[36] Madian M, Ummethala R, El Naga AOA et al (2017) Ternary CNTs@TiO_2/CoO nanotube composites: improved anode materials for high performance lithium ion batteries. Materials 10:678

[37] Tian QH, Tian Y, Zhang W, Huang J, Zhang ZX, Yang L (2017) Impressive lithium storage of SnO_2@TiO_2 nanospheres with a yolk-like core derived from self-assembled SnO_2 nanoparticles. J Alloy Compd 702:99

[38] Chen W, Wei LY, Lin ZY et al (2017) Hierarchical flower-like $NiCo_2O_4$@TiO_2 hetero-nanosheets as anodes for lithium ion batteries. Rsc Adv 7:47602

[39] Shi JW, Chen JW, Cui HJ et al (2012) One template approach to synthesize C-doped titania hollow spheres with high visible-light photocatalytic activity. Chem Eng J 195:226

[40] Cai DD, Li DD, Ding LX, Wang SQ, Wang HH (2016) Interconnected alpha-Fe_2O_3 nanosheet arrays as high-performance anode materials for lithium-ion batteries. Electrochim Acta 192:407

[41] Chaudhari S, Srinivasan M (2012) 1D hollow alpha-Fe_2O_3 electrospun nanofibers as high performance anode material for lithium ion batteries. J Mater Chem 22:23049

[42] Xie KY, Guo M, Lu W, Huang HT (2014) Aligned TiO_2 nanotube/nanoparticle heterostructures with enhanced electrochemical performance as three-dimensional anode for lithium-ion microbatteries. Nanotechnology 25:455401

[43] Xia T, Zhang W, Wang ZH et al (2014) Amorphous carbon-coated TiO_2 nanocrystals for improved lithium-ion battery and photocatalytic performance. Nano Energy 6:109